Taylor & Francis
Taylor & Francis Group

Xenobiotica
the fate of foreign compounds in biological systems

ISSN: 0049-8254 (Print) 1366-5928 (Online) Journal homepage: http://www.tandfonline.com/loi/ixen20

In vitro and *in vivo* pharmacokinetic characterization of mavacamten, a first-in-class small molecule allosteric modulator of beta cardiac myosin

Mark P. Grillo, John C. L. Erve, Ryan Dick, James P. Driscoll, Nicole Haste, Svetlana Markova, Priscilla Brun, Timothy J. Carlson & Marc Evanchik

To cite this article: Mark P. Grillo, John C. L. Erve, Ryan Dick, James P. Driscoll, Nicole Haste, Svetlana Markova, Priscilla Brun, Timothy J. Carlson & Marc Evanchik (2018): *In vitro* and *in vivo* pharmacokinetic characterization of mavacamten, a first-in-class small molecule allosteric modulator of beta cardiac myosin, Xenobiotica, DOI: 10.1080/00498254.2018.1495856

To link to this article: https://doi.org/10.1080/00498254.2018.1495856

Accepted author version posted online: 25 Jul 2018.

In vitro and i*n vivo* pharmacokinetic characterization of mavacamten, a first-in-class small molecule allosteric modulator of beta cardiac myosin

Mark P. Grillo[a], John C. L. Erve[a], Ryan Dick[a], James P. Driscoll[a], Nicole Haste[a], Svetlana Markova[a], Priscilla Brun[b], Timothy J. Carlson[a], and Marc Evanchik[a]

[a]Department of Drug Metabolism and Pharmacokinetics, MyoKardia, Inc., South San Francisco, CA, USA, Phone (650) 741-0900

[b]Sanofi-Aventis Recherche et Développement, 371, Rue du Professeur Joseph Blayac 34184, Montpellier Cedex 04, Phone +33 (0)499774055

Address for Correspondence: Mark P. Grillo, PhD, Drug Metabolism and Pharmacokinetics, MyoKardia, Inc., 333 Allerton Avenue, South San Francisco, CA 94080, Phone 1-650-636-7335, E-mail: mgrillo@myokardia.com

Abstract

1. Mavacamten is a small molecule modulator of cardiac myosin designed as an orally administered drug for the treatment of patients with hypertrophic cardiomyopathy. The current study objectives were to assess the preclinical pharmacokinetics of mavacamten for the prediction of human dosing and to establish the potential need for clinical pharmacokinetic studies characterizing drug-drug interaction potential.

2. Mavacamten does not inhibit CYP enzymes, but at high concentrations relative to anticipated therapeutic concentrations induces CYP2B6 and CYP3A4 enzymes *in vitro*. Mavacamten showed high permeability and low efflux transport across Caco-2 cell membranes. In human hepatocytes, mavacamten was not a substrate for drug transporters OATP, OCT, and NTCP. Mavacamten was determined to have minimal drug-drug interaction risk.
3. *In vitro* mavacamten metabolite profiles included phase I- and phase II-mediated metabolism cross-species. Major pathways included aromatic hydroxylation (M1), aliphatic hydroxylation (M2); *N*-dealkylation (M6), and glucuronidation of the M1-metabolite (M4). Reaction phenotyping revealed **CYPs 2C19 and 3A4/3A5** predominating.
4. Mavacamten demonstrated low clearance, high volume of distribution, long terminal elimination half-life and excellent oral bioavailability cross-species.
5. Simple four-species allometric scaling led to predicted plasma clearance, volume of distribution, and half-life of 0.51 mL/min/kg, 9.5 L/kg, and 9 days, respectively, in human.

Keywords: Cardiac myosin modulator, Mavacamten, MYK-461, drug metabolism, pharmacokinetics, allometric scaling

Introduction

Hypertrophic cardiomyopathy (HCM) is estimated to affect one in 500 individuals of the general population (Maron *et al.* 1995, Semsarian *et al.* 2015). HCM is characterized by cardiac hyper-contractility leading to hypertrophy of the left ventricle, which results in diminished cardiac function (Maron 2002, Gersh *et al.* 2011). HCM results in clinical symptoms at any age, with dyspnoea as the most common manifestation. The disease is associated with chronic and progressive heart failure symptoms, increased risk of atrial fibrillation and associated stroke and an increased risk of malignant ventricular arrhythmias including sudden cardiac death. Approximately 70% of patients with a family history of HCM are known to include point mutations in one of the structural genes of the cardiac sarcomere where 35% to 40% of pathogenic HCM variants are located in the beta cardiac myosin gene (Hershberger *et al.* 2009, Gersh *et al.* 2011). Current pharmaceutical management options for HCM include off-label use of beta-blockers (e.g., metoprolol, propranolol or atenolol) and calcium channel blockers (e.g., verapamil or diltiazem). Other management options include an implantable cardiac defibrillator or invasive septal reduction therapies (to decrease the thickness of the obstructing septum muscle) (Gersh *et al.* 2011).

Mavacamten ((6-([(1S)-1-phenylethyl]amino)-3-(propan-2-yl)-1,2,3,4-tetrahydro-pyrimidine-2,4-dione), formerly MYK-461; Figure 1) is an investigational novel small molecule allosteric modulator of beta cardiac myosin (Green *et al.* 2016) for the treatment of HCM. Mavacamten targets the sarcomere, where it is proposed to both reduce the force of cardiac contractility and facilitate diastolic relaxation in HCM patients. These functions together are thought to lead to improved reduced left ventricular compliance and reduced dynamic left ventricular outflow obstruction in HCM patients. Results from *in vivo* studies in mice

demonstrated that mavacamten mediated the reduction of cardiac myosin sarcomere power output leading to attenuated disease development and progression, which may provide a therapeutic approach to patients with HCM (Green *et al.* 2016).

The objectives of the present work were to characterize the *in vitro* pharmacokinetic properties of mavacamten including absorption, metabolite identification, drug-drug interaction potential, as well as the *in vivo* pharmacokinetics in mice, rats, dogs and monkeys for the prediction of human pharmacokinetics.

Materials and methods

Materials

Mavacamten and authentic metabolite standards (M1 [MYK-2210], M2 [MYK-1078] and M6 [MYK-2241]) were chemically synthesized at MyoKardia, Inc. (South San Francisco, CA, USA) and determined to be at least 99% chemically pure. [^{14}C]Mavacamten (^{14}C incorporation at the pyrimidine-5 carbon atom as indicated in Figure 1), specific activity 51.5 mCi/mmol, 99.7% radiochemically pure, dissolved in ethanol (10 mM), was obtained from Moravek Biochemicals (Brea, CA, USA). The following reagents were obtained from Bioreclamation IVT (Baltimore, MD, USA): plasma and blood (mouse, rat, dog, monkey, human), liver microsomes from mouse (ICR/CD-1, male, pooled), rat (Sprague-Dawley, male, pooled), dog (beagle, male, pooled), cynomolgus monkey (male, pooled) and human (mixed gender, 50-donor pooled); cryopreserved hepatocytes from rat (Sprague-Dawley, male, pooled), dog (beagle, male, pooled), cynomolgus monkey (male, pooled) and human (LiverPool^{TM}, 10-donor, mixed gender); InVitroGRO HT medium and InVitroGRO KHB buffer. cDNA-expressed recombinant human cytochrome P450 (CYP) isoforms (Corning Supersomes) were purchased from Corning (New York, NY, USA).

β-Nicotinamide adenine dinucleotide 2'-phosphate reduced tetrasodium salt hydrate (NADPH), magnesium chloride solution (1 M), dimethyl sulfoxide (DMSO), *N*,*N*-dimethylacetamide (DMA), polyethylene glycol 400 (PEG-400), 2-hydroxypropyl-β-cyclodextrin (2-HP-β-CD) and carbamazepine were purchased from Sigma Aldrich (St. Louis, MO, USA). ORA-Sweet and ORA-Plus were obtained from Perrigo (Allegan, MI, USA). Potassium phosphate buffer (0.1 M, pH 7.4) was purchased from Thermo Fisher Scientific (Waltham, MA, USA). FlowLogicU scintillation fluid was obtained from LabLogic, Inc. (Brandon, FL, USA). Rat studies were performed at Portola Pharmaceuticals (South San Francisco, CA, USA). Mouse, dog and monkey studies were conducted at Xenometrics LLC (Stilwell, KS, USA).

Care and maintenance of animals

All animal procedures were conducted under institutional-approved Institutional Animal Care and Use Committee protocols.

Metabolic stability in liver microsomes across species

Mavacamten (20 mM stock dissolved in DMSO, final concentration of DMSO in the incubation was less than 0.1% [v/v]) was assessed for metabolic stability in liver microsomes from mouse, rat, dog, and human. *In vitro* intrinsic clearance (CL_{int}) was determined as follows. Briefly, incubations (0.3 mL total volume) containing liver microsomes (1 mg protein/mL), NADPH (1 mM), $MgCl_2$ (2.5 mM), mavacamten (1 µM) in potassium phosphate buffer (0.1 M, pH 7.4) were performed at 37 ºC in a shaking benchtop water bath incubator. Incubation aliquots (50 µL) were taken at time 0, 5, 15, 30 and 45 min and added directly to 100 µL of acetonitrile (ACN) containing carbamazepine (20 nM) internal standard. Positive substrate control incubations were

performed with verapamil. Quenched samples were mixed, followed by centrifugation at 4600 rpm for 10 min as described below for the processing of samples from pharmacokinetic studies. The supernatants were analysed by liquid chromatography-tandem mass spectrometry (LC-MS/MS) as described below for the analysis of mavacamten from pharmacokinetic studies. Peak area ratios of mavacamten/carbamazepine from each time point were natural log transformed as the percent remaining relative to time zero (Obach 1999). The slope (*k*) was transformed to an *in vitro* half-life ($t_{1/2}$), where $t_{1/2} = -0.693/k$. The calculated CL_{int} of mavacamten was determined from the relationship $CL_{int} = k$•(volume of incubation in mL/mg microsomal protein)•(mg protein in liver/g liver weight)•(g liver weight/kg body weight). The values for species liver weights and body weights, as well as hepatic blood flows (Q_H) cross species were obtained from Davies and Morris (1993). Values used for liver microsomal protein/liver weight for mouse, rat, and dog were 45 mg/g (Obach 1999) and for human, 33 mg/g. Calculations used for the prediction of hepatic clearance (CL_{pred}) = (Q_H• CL_{int})/(Q_H+ CL_{int}), where the ratio fraction of mavacamten unbound in plasma/incubation (fu_p/fu_{inc} was assumed to equal one in these calculations, where for neutral and basic drugs, fu_p was assumed to cancel out with fu_{inc} (Obach 1999).

A metabolic stability study was conducted in human hepatocytes isolated as described below for mavacamten metabolite identification. Incubations of hepatocytes (1 million viable cells/mL) were performed with mavacamten and positive control substrate verapamil (duplicate incubations per substrate, each 1 µM) over 120 min with outtakes (25 µL) taken at 0, 5, 15, 30, 60 and 120 min and processed for LC-MS/MS analysis as described above for metabolic stability studies in liver microsomes. Predicted *in vivo* hepatic clearance (CL_{pred}) was determined from the apparent hepatocyte *in vitro* clearance

($CL_{int, app}$) estimated from the half-life of drug disappearance. The $CL_{int, app}$ was scaled to *in vivo* units using a scaling factor of 107 million cells/g liver and a liver weight of 26 g liver/body weight. CL_{pred} was calculated based on the well-stirred model with no correction for plasma protein nor non-specific incubation binding.

Plasma protein binding

Fu_p was determined from mouse, rat, dog, monkey and human plasma at concentrations of 0.2, 1 and 10 µM by equilibrium dialysis using a Rapid Equilibrium Dialysis kit (Thermo Scientific, Rockford, IL, USA) per the manufacturer's instructions. Thus, stock solutions of [^{14}C]mavacamten were prepared at 0.04, 1 and 10 mM in ACN. Then 1.35 µL of stock solutions was added to 1350 µL of blank plasma (pH 7.4) from each species in a 96-deep well incubation plate to provide the desired 0.2, 1 and 10 µM incubation concentrations followed by pre-incubation at 37 ºC for 10 min. In triplicate for each concentration tested, [^{14}C]mavacamten in plasma (300 µL) was added to the Rapid Equilibrium Dialysis incubation base plate dialysis inserts (designated as 'red'), followed by the addition of 500 µL of phosphate-buffered saline (pH 7.4) to the buffer side of the base plate inserts (designated as 'clear'). The base plate then was covered with adhesive film followed by incubation with shaking (100 rpm) in a cell culture incubator (37 ºC, 5% CO_2) for 20 h. To determine stability and recovery of drug in plasma, aliquots (100 µL) of plasma from the main incubation plate were taken and added to a 96-shallow well plate, sealed and stored refrigerated at 4 ºC. The incubation plate was also incubated in a cell culture incubator (37 ºC, 5% CO_2) over 20 h for [^{14}C]mavacamten stability/recovery assessment. Post-incubation, 100-µL aliquots of each sample were added to scintillation cocktail and measured for ^{14}C-radioactivity as counts per minute (cpm) on a

LS 6500 Scintillation Counter (Beckman Coulter, Brea, CA, USA). Percent [^{14}C]mavacamten-derived material bound was calculated using the following equation: 100-(100*(cpm_{clear}/cpm_{red})). Recovery was calculated using the following equation:

100•(((300•cpm_{red})+(500•cpm_{clear}))/(300•$cpm_{preincubation}$)).

Blood-to-plasma ratio

The extent of distribution of [^{14}C]mavacamten (rat only) and non-radioactive mavacamten (mouse, rat, dog, cynomolgus monkey and human) between blood cells and plasma was determined using heparinized blood and plasma based on a method adapted from Yu *et al*. (2005). Thus, for each species, pre-warmed blood and plasma (15 min, pH 7.4) were incubated (15 min at 37 ºC) in a 96-deep well plate in triplicate with [^{14}C]mavacamten or non-radioactive mavacamten (1 μM) by adding 5 μL of 200 μM [^{14}C]mavacamten or non-radioactive mavacamten dissolved in DMSO. Then, the 96-well plate containing blood and plasma incubation samples (N=3) was centrifuged in a table-top centrifuge (2000 rpm, 37 ºC, 10 min). Post-centrifugation, 100 μL of supernatant was transferred to a fresh 96-deep well plate followed by the addition of ACN containing carbamazepine internal standard (20 nM, 400 μL). The plate was sealed and mixed by shaking (plate on its side) on an Eberbach Model E6000 mid-range reciprocal shaker (Fisher Scientific, Pittsburgh, PA, USA) at 260 oscillations/sec for 10 min at room temperature. The quenched sample plate was centrifuged (4600 rpm, 10 min, 4 ºC), and aliquots of the resultant supernatants (100 μL) were added directly to scintillation vials containing scintillation fluid and submitted for liquid scintillation counting. Supernatant aliquots (70 μL) from corresponding incubations with non-radiolabelled mavacamten were added to a 96-shallow well plate containing 70 μL of water for LC-MS/MS analysis of mavacamten. The

cross-species mavacamten blood-to-plasma ratios were determined by dividing the concentrations of mavacamten in reference plasma incubation samples by the concentrations in the corresponding plasma supernatants obtained from centrifugation of blood incubation samples.

Permeability in Caco-2 cells

Cell permeability and the efflux potential of mavacamten were investigated in a Caco-2 cell line. Briefly, cells were seeded (density of $6.9x10^5$ cells/mL) in culture medium (Hank's balanced salt solution, 25 mM HEPES, pH 7.4) in Corning Transwell® plates (96-well, polycarbonate membrane, 0.4-µm pore size, 0.14 cm2 growth area, Corning, Corning, NY, USA) and cultivated (cell culture incubator at 37 °C, 5% CO_2, 95% relative humidity) for 14-18 days with feeding at two-day intervals. For apical to basolateral (A>B) permeability, mavacamten (1 µM) was added to the apical (A) side and amount of permeation was determined on the basolateral (B) side; for basolateral to apical (B>A) permeability, mavacamten (1 µM) was added to the B side and the amount of permeation was determine on the A side. Caco-2 cells were incubated for 2 h and the receiver side buffer removed for analysis of mavacamten by LC-MS/MS. Trans-epithelial electrical resistance (TEER) and lucifer yellow leakage were employed to confirm monolayer integrity at the beginning and end of the experiments, respectively. Data are expressed as permeability (P_{app}):

P_{app} = (dQ/dt)/(C_0•A), where dQ/dt is the rate of permeation, C0 is the initial concentration of mavacamten, and A is the monolayer area. In the bi-directional permeability studies, the efflux ratio (R_E): $R_E = P_{app}$ (B→A)/P_{app} (A→B), where R_E >2 indicates potential efflux by transporters such as P-glycoprotein (P-gp).

Evaluation of the uptake of mavacamten by cryopreserved human hepatocytes in primary culture

Uptake into plated hepatocytes was measured by the method described by Poirier *et al.* (2008). Thus, cryopreserved human hepatocytes were obtained from three individual donors obtained from Invitrogen (Carlsbad, CA, USA) and InVitro ADMET Laboratories, LLC (Columbia, MD, USA). Mavacamten (0.5, 3, 10, 30, 50, 80 and 100 μM) was incubated with human hepatocytes at 37°C in the presence and in the absence of an 'inhibitor cocktail' for 3 min. The 'inhibitor cocktail' consisted of the potent transporter inhibitors cyclosporine A (20 μM), rifampicin (20 μM) and quinidine (100 μM). Mavacamten concentration was determined by LC-MS/MS. The uptake into the hepatocytes was normalized by the protein amount in each well (mg/well) and incubation time to give pmol/min/mg protein. The increase in uptake into hepatocytes was calculated by dividing the uptake at 37 °C by background uptake according to the following equations: Uptake at 37 °C divided by uptake at 37 °C in the presence of the inhibitor cocktail; increase in hepatic transport = Q(37 °C minus inhibitor cocktail) / Q(37 °C plus inhibitor cocktail), where Q is the quantity of compound (pmol) transported into a certain amount of cells (mg) at the end of an incubation period (min) expressed in pmol/min/mg protein units. All results expressed as mean ± standard error of the mean.

Metabolite identification in hepatocyte suspensions cross-species

The *in vitro* metabolite profiles of [^{14}C]mavacamten cross-species in hepatocyte suspensions were obtained following incubations (4 h) with rat, dog, cynomolgus monkey and human cryopreserved hepatocytes. Hepatocyte suspension incubations were performed as follows: prior

to thawing hepatocytes, reagents InVitroGRO HT and KHB media were pre-warmed to 37 °C in a water bath. Hepatocyte vials then were retrieved from cryopreservation (<−140°C, liquid nitrogen) storage, uncapped and quickly warmed in a 37°C water bath. Once thawed (2 min), hepatocytes were transferred to culture tubes containing 50 mL InVitroGRO HT (thawing) medium. The culture tubes were capped and gently inverted (4–6 times) and centrifuged (100*g*, room temperature, 5 min). Following centrifugation, supernatants were discarded and pellets were gently re-suspended using 2 mL pre-warmed KHB buffer. Cell counts and viability determinations were assessed by trypan blue exclusion testing with measured viability ranging from 80% to 90%. Cell suspensions were further diluted with KHB buffer to obtain a cell concentration of 1 million viable cells/mL. Hepatocyte incubations were performed in 20-mL glass scintillation vials with 3-mL aliquots of cell suspensions from each species incubated separately and metabolism of substrates initiated by the addition of 3 μL of [^{14}C]mavacamten (10 mM in ethanol) stock to provide a final [^{14}C]mavacamten concentration of 10 μM. Incubations were performed in loosely capped vials in a humidified cell culture incubator (5% CO_2, 95% air, 37 °C) with gentle mixing. Aliquots (1 mL) were taken at time zero and after 4 h of incubation and quenched with ACN (1.7 mL). Quenched incubations extracts were stored frozen (−20 °C) until processing as described above for subsequent LC/radioactivity and LC-MS/MS analyses as described below.

LC-MS/MS analysis for metabolites

Extracts from *in vitro* incubations of mavacamten or [^{14}C]mavacamten with hepatocytes or recombinant human CYP enzymes were characterized by LC-MS/MS. The LC-MS/MS systems used to detect and identify metabolites included an AB Sciex 5500 Q-Trap (AB Sciex, Foster

City, CA, USA) coupled with an Aria LX-2 multiplex system (Thermo Fisher Scientific, Waltham, MA, USA); a Thermo Scientific LTQ Orbitrap-Velos (Thermo Fisher Scientific) coupled to an Accela UHPLC pump and autosampler (Thermo Fisher Scientific); a Thermo Electron LTQ Orbitrap XL mass spectrometer coupled with a Dionex UltiMate 3000 UHPLC containing in-line diode array detection and an OAS-3300TXRS autosampler; and a Q-Exactive mass spectrometer (Thermo Scientific, Bremen, Germany). LC-MS/MS analysis on the 5500 Q-Trap was performed in the positive ion electrospray mode with a curtain gas of 20, high collision gas, ion spray voltage of 5500, temperature of 700 ºC, ion source gas 1 and 3 of 60, a de-clustering potential of 120, exit potential 10 and a collision energy of 30–40 (when applicable). Analysis using the LTQ Orbitrap-Velos was in the positive ion mode with an HESI-2 source and a capillary temperature of 350 ºC, a source heater temperature 345 ºC with sheath gas, auxiliary gas and sweep gas flows of 50, 12 and 5, respectively. A source voltage of 3500 and a source current of 100 were used together with an S-lens RF level of 1. Data-dependent scans were utilized with dynamic exclusion and wideband activation that collected the MS/MS, MS^3 and MS^4 spectra of the two most abundant masses of the Fourier transform (FT) high-resolution (resolution 15,000) full-scan spectrum. The Orbitrap mass analyser was calibrated according to the manufacturer's directions using a mixture of caffeine, MRFA peptide and Ultramark before use. Survey scan MS data (from *m/z* 100–1200) were acquired in the Orbitrap with a resolving power of 70K (at *m/z* 400). For MS/MS experiments on the Orbitrap LC-MS/MS, ions of interest were isolated with a 3-Da isolation width, collision-induced dissociation (conducted via higher-energy C-trap dissociation [HCD]) with an activation q of 0.25 and an activation time of 30 ms with normalised collision energy from 10% to 35%. The resulting product ions were measured with resolving power from 7.5K. Full-scan MS data

was examined manually to look for known and possible metabolic transformations of the drug. Data acquisition and processing were performed using Xcalibur software (version 2.0.7, Thermo Fisher Scientific, Inc.). The Thermo Electron LTQ Orbitrap XL mass spectrometer used electrospray ionization employed in the positive ion mode with the needle potential held at 5.01 kV, a sheath flow rate of 35.02, aux flow rate of 9.99, a current of 2.6 µA, a capillary temperature of 325 ºC and a capillary voltage of 15.99. Vacuum conditions were an ion gauge pressure of $2.33x10^{-5}$ Torr and a convection gauge pressure of 0.90 Torr. Positive-ion mode full scan (*m*/*z* 100 to *m*/*z* 1000) LC-MS analysis was conducted with a scan time of 0.73 sec and source collision energy of 10 V. The tandem MS/MS conditions used were 2 mTorr helium collision gas and a collision potential of 35 eV. Xcalibur software (version 2.1.0, Thermo Fisher Scientific) was used to acquire all data. The Q-Exactive mass spectrometer was operated in positive mode with a spray voltage of 3.5–3.9 kV for ionization. Sheath and auxiliary gas were set at 50 and 5, respectively. The probe heater and capillary were maintained at 360°C and 200°C, respectively. The S-lens RF level was set at 50, and the collision gas pressure was approximately 1.3 mTorr. Chromatographic separation was achieved with a Betabasic C18 column (4.6 x 250 mm, 3 µm) (Thermo Scientific, San Jose, CA, USA). The sample chamber in the autosampler was maintained at 5 °C, while the column temperature was at 30°C. The mobile phase consisted of 0.1% formic acid in water (solvent A) and 0.1% formic acid in ACN (solvent B) and was delivered at 700 µL/min. For the analysis of sample extracts derived from *in vitro* metabolite identification studies in hepatocytes, the initial solvent composition consisted of 5% solvent B, and after 2 min a linear gradient increased to 45% solvent B over 40 min, then to 85% solvent B over 3 min and maintained for 6 min, followed by a decrease to 5% solvent B over 4 min while maintaining this composition for 10 min for a total run time of 62 min.

LC/Radiochromatography

Radiochromatograms were collected using a β-RAM radio flow detector (Model 5, LabLogic, Inc., Brandon, FL, USA) connected to an Agilent 1200 Binary SL HPLC pump (Agilent Technologies, Santa Clara, CA, USA) and CTC Analytics PAL autosampler (LEAP Technologies, Carrboro, NC, USA). The *β*-RAM5 was equipped with a 200 µL flow cell and operated in Active Counting Mode with a default scintillation flow rate of 2.00 mL/min. Data were processed and exported using Laura 4 software (LabLogic, Inc., Brandon, FL, USA). Quenched hepatocyte incubation aliquots were vortex mixed followed by micro-centrifugation (13,000 rpm, 10 min, 4 ºC). Supernatants then were transferred to clean Eppendorf micro-centrifuge tubes and partially dried down by vacuum centrifugation. The remaining supernatant was then diluted 3-fold with water and transferred to a glass high-performance liquid chromatography vials for analyses by LC/radiochromatography and LC-MS/MS. The processed samples were stored at -70°C until analysis. Incubation extracts were chromatographed on a reverse-phase column (BetaBasic-18, 250 x 4.6 mm, 3 µ, (Thermo Fisher Scientific, Waltham, MA, USA) with a flow rate of 0.7 mL/min over 62 min. The gradient aqueous mobile phase (solvent A) consisted of 0.1% formic acid in water (v/v) in water, and the organic mobile phase (solvent B) contained ACN with 0.1% formic acid (v/v). Elution was achieved by holding the aqueous solvent A mobile phase constant at 95% for 2 min and then, in a linear fashion, decreasing to 55% solvent A to 42 min of elution followed by a further decrease in solvent A to 15% at 51 min then a rapid increase to 95% solvent A (over 1 min) to 52 min and finally 10 min of equilibration at 95% solvent A prior to further analyses.

CYP450 reaction phenotyping

CYP450 reaction phenotyping studies with mavacamten were performed with human recombinant CYP Supersomes (isoforms 1A2, 2B6, 2C8, 2C9*1 [wild-type], 2C19, 2D6*1 [wild-type], 2E1, 3A4, 3A5). Incubations were performed with 1 μM mavacamten incubated with 150 pmol/mL enzyme and NADPH (1 mM) for 1 h (37 °C). The amount of mavacamten remaining relative to the NADPH-deficient control was determined by LC-MS/MS analysis as described above. In addition, metabolites of mavacamten (M1, M2 and M6) were assessed for products of each of the recombinant enzymes. Mavacamten reaction phenotyping for metabolite identification was conducted from scaled-up incubations with selected recombinant human CYP Supersomes and analysed by LC-MS/MS accurate mass hybrid FT ion trap detection as described above. Thus, mavacamten was incubated (40 μM, 60 min, 37°C, 1 mM NADPH) with selected recombinant human CYP isoforms (150 pmol/mL 2C9*1, 2C19, 3A4 and 3A5).

CYP inhibition studies

A series of studies was conducted to determine the CYP450 drug-drug interaction potential of mavacamten as measured by competitive inhibition potential in human microsomes.

CYP isoforms (and specific probe substrates) tested were 1A2 (phenacetin), 2B6 (bupropion), 2C9 (diclofenac), 2C19 (*S*-mephenytoin), 2D6 (dextromethorphan), and 3A4/A5 (testosterone, midazolam). Standard methods (Walsky and Obach 2004) were used to investigate the inhibition potential of mavacamten up to 100 μM test article. Results expressed as IC_{50} (half-maximal inhibitory concentration).

CYP induction studies

The study was designed to assess the potential of test article mavacamten to induce CYP isoforms 1A2, 2B6 and 3A4 mRNA levels and enzymatic activity using primary cultured human hepatocytes. The study was conducted in accordance with Discovery Labware SOP mWB-CR-046 and other documented procedures. **Data from three separate donors of cryopreserved hepatocytes were used for CYP1A2, CYP2B6, and CYP3A4 induction.** Hepatocytes plated on collagen I-coated 96-well plates were exposed to the mavacamten for a total of three days, with a medium change approximately every 24 h. Induction of CYP1A2, CYP2B6 and CYP3A4 was measured by mRNA expression assays selective for each CYP isoform by real time reverse transcription polymerase chain reaction analysis. Induction of *in situ* catalytic activity was determined for CYP1A2, CYP2B6 and CYP3A4 using specific probe substrates. **To estimate half-maximal effective concentration (EC_{50}) and maximal effect (E_{max}) values, concentration-response fold-induction versus vehicle control data were fit to a sigmoidal dose-response one-site fit model. Positive control CYP inducers used were omeprazole (CYP1A2, 50 µM), phenobarbital (CYP2B6, 1000 µM), and rifampicin (CYP3A4, 10 µM).**

Pre-clinical species pharmacokinetic studies

Mavacamten was administered as the free base and formulated in DMA:PEG-400:30% 2-HP-β-CD (5:25:70) at 1 mg/mL and dosed at 1 mg/kg for both intravenous (via mouse tail vein, rat femoral vein) and oral administration (oral gavage, 5 mL/kg) to mice (n=3, fed) and at 1 mg/kg intravenous and 2 mg/kg oral for rat (n=3, fed). The pharmacokinetic parameters of mavacamten were estimated in male beagle dogs (n=3, fed) following a single intravenous (via cephalic vein) or single oral dose of 0.25 and 0.5 mg/kg, respectively. The oral dose (oral gavage, 5 mL/kg) was formulated as a suspension in 0.5% methylcellulose, and the intravenous dose was formulated in

DMA:PEG400:0.9% saline (5:10:85; v:v:v). The pharmacokinetic parameters of mavacamten were estimated in male cynomolgus monkeys (n=3, fed) following a single intravenous (via cephalic vein) or single oral gavage dose at 0.25 and 0.5 mg/kg (1 mL/kg), respectively. The intravenous dose was formulated in DMA:PEG400:0.9% saline (5:10:85), and oral dose was formulated as suspension in ORA-Sweet: ORA-Plus (50:50).

Pharmacokinetic studies (in-life portion) were conducted at Xenometrics, LLC (Stilwell, KS, USA) for experiments in mice, dog and monkey, and rat pharmacokinetic studies were performed at Portola Pharmaceuticals (South San Francisco, CA, USA). For studies in mice (male C57BL6), blood collection (cardiac puncture, approximately 0.5 mL) was performed at pre-dose, 0.0833, 0.166, 0.5, 1, 2, 4, 8 and 24 h post-dose for intravenous and at pre-dose, 0.166, 0.5, 1, 2, 3, 4, 8 and 24 h post-dose for oral administration. **For studies in rat (male Sprague-Dawley), blood collection (collected via jugular vein catheter, approximately 0.3 mL) was performed at pre-dose, 0.033, 0.167, 0.5, 1, 2, 4, 6, 8 and 24 h post-dose for intravenous and at pre-dose, 0.25, 0.5, 1, 2, 3, 6.75, 8 and 24 h post-dose for oral administration. For studies in dog (male beagle), blood collection (obtained from the saphenous vein, approximately 1.5 mL) was performed at pre-dose, 0.0833, 0.25, 0.5, 1, 2, 4, 8, 16, 24, 48, 72, 96, 120, 144 and 168 h post-dose for intravenous and at pre-dose, 0.25, 0.5, 1, 2, 3, 4, 8, 16, 24, 48, 72, 96, 120, 144 and 168 h post-dose for oral administration. For studies in monkey (male cynomolgus), blood collection (obtained from the saphenous vein, approximately 1.5 mL) was performed at pre-dose, 0.083, 0.5, 1, 4, 8, 24, 72,120,168, 240 and 336 h post-dose for intravenous and at pre-dose, 0.25, 0.5, 1, 2, 4, 8, 24, 48, 72, 96, 120 and 144 h post-dose for oral administration.** For each species, blood samples were collected in K_2EDTA-containing

tubes and centrifuged to collect plasma. Plasma was frozen at −20 ºC (mouse, rat and dog) or −70 ºC (monkey) until further processing for mavacamten quantitation.

Routes of elimination in rat

The excretion of [^{14}C]mavacamten-derived radioactivity was investigated at Covance Laboratories Inc. (Madison, WI, USA) in bile duct-cannulated (BDC) male Sprague-Dawley (SD) rats (n=4) following single dose intravenous administration (1 mg/kg). The dose was prepared in a formulation containing DMA:PEG-400:2-HP-β-CD 30% (w:v) in water 5:25:70 (v:v:v). Urine and feces were collected in glass containers surrounded by dry ice pre-dose, at 0-6 h and 6-24 h post-dose, and at 24 h intervals through 96 h post-dose. Bile was collected in glass containers surrounded by dry ice pre-dose, at 0-2, 2-6, and 6-24 h post-dose, and at 24 h intervals through 96 h post-dose. Animals were sacrificed with an overdose of isoflurane anesthesia and the residual carcass from each animal was weighed and retained for radioanalysis. Excreta were analyzed for radioactivity by liquid scintillation counting. LC/Radiometric detection, the same method as employed for LC/radiometric detection for *in vitro* metabolism studies, was used for the analysis of extracts of AUC-pooled (neat, 0-96 h, microcentrifuged) urine and bile.

Bioanalytical LC-MS/MS analysis

In general, thawed plasma samples (50 µL) obtained from pharmacokinetic studies were transferred to a 96-deep well plate (1 mL, round bottom, Corning Inc., Fremont, CA, USA) and processed by the addition of ACN solution (300 µL) containing carbamazepine (20 nM). The plate was sealed with a storage mat and followed by shaking the plate on its side on an Eberbach

Model E6000 mid-range reciprocal shaker (Fisher Scientific, Pittsburgh, PA, USA) at 260 oscillations/second for 10 min at room temperature. After shaking quenched mixture, the sample plates were centrifuged on an Allegra X-15R centrifuge (Beckman Coulter, Brea, CA, USA) at 4600 rpm at 4 ºC for 10 min. Post-centrifugation, aliquots (20 µL) of supernatants were added to separate 96-shallow well PP assay plates, (V-bottom, 200 µL, Corning Inc., Fremont, CA, USA) followed by the addition of 120 µL of HPLC-grade water to each well. The plates then were foil sealed (Axygen easy pierce heat sealing film, Fisher Scientific, Pittsburgh, PA, USA) with an Axygen PlateMax semi-automated plate sealer (Axygen Scientific, Union City, CA, USA) prior to LC-MS/MS analysis. Extracts from *in vivo* pharmacokinetic studies were injected onto a Hypersil Gold AQ 5 um 20 x 2.1 mm DASH HTS analytical column (Thermo Scientific, Waltham, MA, USA) at room temperature.

The LC-MS/MS system consisted of a Transcend 1250 pump and a LX-2 Thermo Cohesive duplexing apparatus (Thermo Scientific, Waltham, MA, USA) linked to a CTC PAL auto-injector (Leap Technologies, Carrboro, NC, USA) and QTRAP 5500 mass spectrometer (AB Sciex, Foster City, CA, USA). Mavacamten concentrations in plasma sample extracts were determined using reverse-phase liquid chromatography with a solvent system consisting of 0.1% formic acid in water (mobile phase A) and ACN with 0.1% formic acid (mobile phase B). A gradient of mobile phase B increased from 10% to 85% over 30 sec at a flow rate of 0.9 mL/min. Detection of mavacamten and the internal standard, carbamazepine, was achieved in the positive ion mode (IonSpray voltage of 5500 V, TurboIonSpray temperature of 600 ºC, curtain gas setting at 40, collision-activated dissociation gas setting at medium and nebulizing and auxiliary gas settings at 75) by multiple reaction monitoring for the transition MH^+ *m/z* 274.0–128.0

(mavacamten) and MH^+ *m/z* 237.0–194.0 (carbamazepine). Samples were quantified against a calibration curve spanning a 1000-fold concentration range (2–2000 ng/mL).

Pharmacokinetic analysis

Peak areas for mavacamten and carbamazepine were obtained using Analyst 1.6 (AB Sciex, Foster City, CA, USA), and the peak area ratio (mavacamten/internal standard) was used for quantitation. Calibration curve data was fit using linear regression and $1/x^2$ or 1/x weighting. Reported plasma concentrations-versus-time data for mavacamten were analysed to determine pharmacokinetic parameters using non-compartmental modelling in Phoenix WinNonlin version 6.3. (Pharsight, Mountain View, CA, USA). Pharmacokinetic parameters calculated from intravenous dosing studies including the area under the concentration-time curve (AUC) from time 0 h to infinity ($AUC_{0\text{-}inf}$), plasma clearance (CL_p), steady-state volume of distribution (Vd_{ss}) and terminal elimination $t_{1/2}$. Pharmacokinetic parameters calculated directly from concentration-time data from oral dosing studies included the maximum observed concentration in plasma (C_{max}) and the time of C_{max} (T_{max}).

Simple allometric scaling of pre-clinical in vivo clearance and volume of distribution for human pharmacokinetics prediction

Assuming a one-compartment model, simple allometric scaling (Boxenbaum 1982) was applied using mean pharmacokinetic parameters of unbound CL and unbound Vd_{ss} for mavacamten from intravenous pharmacokinetic studies in mouse, rat, dog and cynomolgus monkey, which were correlated to corresponding body weight (BW) using the power equation $Y = a \bullet BW^b$, where *a* and *b* are coefficient and exponent, respectively. Least square

fitting of log BW versus log *Y* allowed for estimates of exponents and coefficients. Mouse, rat, dog, cynomolgus monkey and human body weights of 0.02, 0.25, 10, 5 and 70 kg, respectively, were assumed. Correction for maximum life span potential (MLP) was also examined based on the 'rule of exponents' (Mahmood and Balian 1996), where simple allometric scaling of unbound blood clearance multiplied by corresponding MLP (Nagilla and Ward 2004, Tang and Mayersohn 2005) obtained from each species (mouse, 2.8; rat, 5.3, dog, 18.4; monkey, 22.9 years) was performed as above to provide an allometric scaled CL•MLP in human followed by correction for human MLP (93.4 years). A simpler species liver blood flow method (Ward and Smith 2004) was also used to predict human mavacamten clearance. By this method, the intravenous clearance from a pre-clinical species, as a percentage of liver blood flow (Q) was used to predict human clearance ($CL_{human} = CL_{animal} \bullet (Q_{human}/Q_{preclinical\ species})$). **Assuming a one-compartment model, the predicted $t_{1/2}$ of mavacamten in human was calculated using the predicted pharmacokinetic parameters ($t_{1/2} = Vd_{ss} \bullet 0.693/CL$).**

Results

Metabolic stability in liver microsomes across species

Metabolic stability studies in liver microsomes across species in mouse, rat, dog and human were conducted to attempt to model the hepatic clearance rate of mavacamten. CL_{pred} and *in vitro* $t_{1/2}$ values calculated from the slope of ln (% mavacamten remaining) in incubations versus incubation time are presented in Table 1. The disappearance of mavacamten from incubations with each species liver microsomes was low and did not exceed a threshold of 20% disappearance after 45 min of incubation (incubation half-life >124 min). Therefore,

the CL_{pred} from plasma (CL_p) *in vivo* in for mouse, rat, dog, and human were designated as <16.3, <10.6, <8.8, and <4.9 mL/min/kg, respectively. These high *in vitro* metabolic stability results are consistent with the observed low CL_p determined from intravenous pharmacokinetic studies in pre-clinical species as described below.

Results from metabolic stability assessment in human hepatocytes showed no detectable clearance of mavacamten (incubation $t_{1/2}$ >700 min, CL_{pred} <2.4 mL/min/kg); whereas the observed clearance of the CYP3A4 substrate verapamil (incubation $t_{1/2}$ 46 min, CL_{pred} =14 mL/min/kg) (data not shown) indicating metabolically functional human hepatocytes.

Plasma protein binding

Plasma protein binding of [^{14}C]mavacamten was consistently high across species and ranged from 83.9% bound in mouse to 95.1% bound in monkey (Table 1). Within species, no significant concentration effects were observed in the concentration range (0.2–10 μM) evaluated. Binding of mavacamten to mouse plasma protein was lower than in other species examined and was approximately 10% lower than in human plasma. Recovery of [^{14}C]mavacamten after 20 h of incubation was approximately 85% across species.

Blood-to-plasma ratio

The blood-to-plasma ratio of [^{14}C]mavacamten in rat blood was determined to be 0.80 ± 0.04, which was consistent with the blood-to-plasma ratio obtained by LC-MS/MS analysis of extracts of samples from a separate experiment of rat blood with non-radioactive mavacamten (0.82 ± 0.11, Table 1). **Blood-to-plasma ratios across species were not significantly different,**

ranging from 0.72–0.82, indicating a lack of distribution of drug into blood cells, and that pharmacokinetic parameters based on plasma analysis are representative of blood pharmacokinetics.

Permeability in Caco-2 cells

Cell permeability and efflux potential of mavacamten were investigated in the Caco-2 cell line at a concentration of 1 µM. The mean apparent permeability observed in both the A-to-B and B-to-A directions was measured to be 24.7 and 38.3 x 10^{-6} cm/sec, respectively, with an efflux ratio (R_E) of 1.6. These data indicate high permeability and low potential of efflux transport occurring *in vivo* for mavacamten. Results for positive control compounds digoxin (5 µM, $P_{app\ (A-B)}$=0.76; $P_{app\ (B-A)}$=25.2; R_E=33.2) and propranolol (5 µM, $P_{app\ (A-B)}$=26.4; $P_{app\ (B-A)}$=20.7; R_E=0.8), tested in the same permeability assay, were consistent with their known permeability and efflux ratio properties.

Evaluation of the uptake of mavacamten by cryopreserved human hepatocytes in primary culture

In order to assess the pathway for mavacamten uptake into hepatocytes, increasing concentrations of mavacamten (from 0.5–100 µM) were incubated for 3 min in the absence and in the presence of a transporter 'inhibitor cocktail' at 37 °C with three different cryopreserved human hepatocytes batches. In the concentration range of 0.5–30 µM, mavacamten uptake was not markedly different after 3 min at 37 °C in the absence compared to the presence of the transporter 'inhibitor cocktail', i.e., mean uptake ratios between 1.2 and 1.5-fold were observed (Table 2). Therefore, mavacamten cannot be clearly identified as a

substrate of organic-anion-transporting polypeptides, organic cation transport proteins and Na^+-taurocholate co-transporting polypeptides in the concentration range tested. Incubation precipitates were observed at 50, 80 and 100 μM mavacamten, and therefore, data from incubations at these concentrations were not used to determine CL_{diff} of mavacamten. Mavacamten showed a CL_{diff} ranging from 10.2–14.2 μL/min/mg protein in the three different human hepatocyte donors tested.

CYP inhibition and induction

Mavacamten did not inhibit CYPs 1A2, 2B6, 2C9, 2C19, 2D6 or 3A4/5 at any concentration tested (IC_{50} >30 μM). Positive control compounds produced CYP inhibition consistent with published results (Walsky and Obach 2004): 1A2 (furafylline IC_{50} 2.24 μM), 2B6 (clopidogrel IC_{50} 0.011 μM), 2C9 (sulfaphenazole IC_{50} 0.302 μM), 2C19 (ticlopidine IC_{50} 0.73 μM), 2D6 (quinidine IC_{50} 0.012 μM), and 3A4/5 (ketoconazole IC_{50} 0.01 μM [testosterone]; 0.009 μM [midazolam]). Results from CYP induction studies conducted in cryopreserved human hepatocytes from three different donor preparations showed mavacamten to induce both mRNA levels and enzyme activities of CYP2B6 and CYP3A4 enzymes in a concentration-dependent fashion (Table 3). In both the mRNA and enzyme activity assays testing the isoforms CYP1A2, CYP2B6 and CYP3A4, positive control inducers exhibited at least a 4.5-fold increase relative to vehicle control in each hepatocyte lot tested. Treatment with mavacamten at concentrations of 0.05–15 μM resulted in no induction of CYP1A2 mRNA expression or activity but caused concentration-dependent induction of mRNA expression and enzyme activity of both CYP2B6 and CYP3A4, with maximal induction responses over 2-fold and greater than 20% of positive control responses. Both E_{max} and EC_{50}

values are shown in Table 3 for CYP2B6 and CYP3A4 mRNA and enzyme activity measurements.

Metabolite identification in hepatocyte suspensions cross-species

Metabolite LC/radiometric chromatographic profiles of [^{14}C]mavacamten obtained from analysis of extracts from 4 h of incubations with rat, dog, monkey and human cryopreserved hepatocytes are shown in Figure 2. Results showed mavacamten to be the major peak detected by LC/radiometric analysis cross-species, and metabolites observed in human hepatocyte incubation extracts were also detected from rat, dog and monkey hepatocyte mavacamten incubation extracts. Three identified metabolites of mavacamten were detected by LC/radiometric analysis from human hepatocyte incubation extracts, namely, M1, M2 and M6, and accounted for 0.78, 0.94 and 0.77% of the total radioactivity, respectively (Table 4).

LC-MS/MS analysis of metabolites of mavacamten

The metabolites of [^{14}C]-labelled and unlabelled mavacamten detected from incubations with hepatocytes were characterized and their chemical structures determined by tandem LC-MS/MS analysis. Tandem mass spectra of mavacamten and metabolites (M1, M2, M4, M6, M10, M11 and M13) detected in hepatocyte incubation extracts, including informative mass spectrometric evidence for each of the metabolites detected, are described below. A scheme for the metabolism of mavacamten in hepatocytes is shown in Figure 3.

Identification of mavacamten metabolites

Reverse-phase LC/radiometric analysis of [^{14}C]mavacamten showed it to elute at a retention time of 38.5 min (Figure 2A). Corresponding high-resolution LC-MS/MS provided an $[M+H]^+$ ion at *m/z* 276.1572 and major fragment ions at *m/z* values 105.0695, 130.0484, 172.0953 and 234.1110 proposed to be formed as indicated in Figure 4A. The origin of these fragment ions is described below for the corresponding LC-MS/MS analysis of the non-radiolabelled derivative. Thus, using a different LC/MS gradient elution method, mavacamten eluted with a retention time of 46.4 min (LC-MS chromatogram not shown) and displayed a protonated molecular ion ($[M+H]^+$) at *m/z* 274.1562, which is consistent with the elemental composition $C_{15}H_{19}N_3O_2$ (mass error 1.1 ppm). Tandem mass spectrometric analysis of mavacamten by collision-induced dissociation of the parent protonated molecular ion provided a loss of the isopropyl side-chain from the molecular ion generating *m/z* 232 (Supplemental Online Material Figure 1). Cleavage of the carbon-amino-nitrogen bond with charge retention on the phenylethyl ring generated *m/z* 105. Cleavage of the carbon-amino-nitrogen bond with charge retention on nitrogen generated amino *N*-isopropyl pyrimidinedione with *m/z* 170, which underwent further fragmentation through loss of the isopropyl side chain to form *m/z* 128. Simultaneous cleavage of both the carbon-amino- nitrogen bond and cleavage through the pyrimidinedione ring with loss of the *N*-isopropyl group generated the product ion at *m/z* 85.

Metabolite M1 (MYK-2210)

Metabolite M1 was detected in LC/radiochromatograms from all incubations except dog hepatocyte extracts. Reverse-phase LC/radiometric analysis showed metabolite M1 to elute at retention time 29.5 min (Figure 2A). Corresponding high-resolution LC-MS/MS analysis provided an $[M+H]^+$ ion at *m/z* 292.1526 and major fragment ions at *m/z* values 121.0645,

130.0483 and 172.0952 proposed to be formed as indicated in Figure 4B. The origin of these fragment ions is described for the corresponding LC-MS/MS analysis of the non-radiolabelled derivative in Supplemental Online Material Figure 2. M1 was shown to have identical retention time and product ion spectrum compared with authentic 3-isopropyl-6-((1-4-hydroxyphenylethyl)amino)pyrimidine-2,4(1H,3H)-dione (data not shown). Thus, M1 was identified as 4-hydroxyphenyl-mavacamten (MYK-2210).

Metabolite M2 (MYK-1078)

Metabolite M2 was detected in radiochromatograms from all incubations except from dog hepatocytes. Reverse-phase LC/radiometric analysis showed metabolite M2 to elute with a retention time of 31.9 min (Figure 2A) and to co-elute with authentic M2 (MYK-1078) standard (data not shown). Corresponding high-resolution LC-MS/MS analysis provided an $[M+H]^+$ ion at *m/z* 292.1526 and major fragment ions at *m/z* values 105.0696, 130.0485, 170.0795, 188.2376 and 234.1104 proposed to be formed as indicated in Figure 4C. The origin of these fragment ions is described for the corresponding LC-MS/MS analysis of the non-radiolabelled derivative in Supplemental Online Material Figure 3. Tandem LC-MS/MS of M2 showed an identical retention time and product ion mass spectrum compared with authentic 3-hydroxy isopropyl-6-((1-phenylethyl)amino)pyrimidine-2,4(1H,3H)-dione (data not shown). Thus, M2 was identified as 3-hydroxy-isopropyl-mavacamten (MYK-1078).

Metabolite M4

Metabolite M4 was observed only in radiochromatograms from rat hepatocyte incubations where it was the major metabolite detected. Reverse-phase LC/radiometric analysis showed metabolite

M4 to elute with a retention time of 23.9 min (Figure 2A). Corresponding high resolution LC-MS/MS analysis provided an $[M+H]^+$ ion at *m/z* 468.1835 and major fragment ions at *m/z* values 121.0644, 130.0483, 172.0952, 250.1055 and 292.1523 proposed to be formed as indicated in Figure 4D. The origin of these fragment ions are described for the corresponding LC-MS/MS analysis of the non-radiolabelled derivative as shown in Supplemental Online Material Figure 4. Thus, M4 was identified as the ether-linked glucuronide of metabolite M1.

Metabolite M6

Metabolite M6 was detected in radiochromatograms from all hepatocyte incubation extracts. Reverse-phase LC/radiometric analysis showed metabolite M6 to elute with a retention time of 15.8 min (Figure 2A). Corresponding high-resolution LC-MS/MS analysis provided an $[M+H]^+$ ion at *m/z* 172.0956 and major informative fragment ions at *m/z* values 87.0425 and 130.0484, proposed to be formed as indicated in Figure 4E. The origin of these fragment ions is described in Supplemental Online Material Figure 5 for the corresponding LC-MS/MS analysis of the non-radiolabelled derivative. M6 had an identical retention time and product ion spectra as authentic 3-isopropyl-6-(amino)pyrimidine-2,4(1H,3H)-dione (MYK-2241) (data not shown).

Metabolite M10

Metabolite M10 was detected, but not fully characterized, from rat hepatocyte extracts only. LC/radiometric analysis showed metabolite M10 to elute at a retention time of 43.2 min (Figure 2A). LC/MS analysis of [^{14}C]M10 provided an $[M+H]^+$ ion at *m/z* 362. The LC-MS/MS characterization of metabolite M10 is described below regarding the corresponding non-radiolabelled derivative. The observed accurate mass (*m/z* 360.1922) of

the unlabelled analogue is in close agreement (Δ=0.387 ppm) with a calculated mass of *m/z* 360.1918 for $C_{19}H_{26}O_4N_3$. This corresponds to a net addition of the elements of $C_4H_6O_2$ (*m/z* 86.0368) to mavacamten. Metabolite M10 provided structurally informative MS/MS, MS^3 and MS^4 spectra (Supplemental Online Material Figure 6). Based on the observed fragment ions, the metabolic transformation is proposed to be located on the uracil-moiety, and not on the ethylbenzene moiety, since, similar to mavacamten, cleavage of the carbon-nitrogen bond resulted in the ethylbenzene fragment ion *m/z* 105 ion. In addition, MS^4 fragmentation of the MS^3 *m/z* 239 ion containing the uracil moiety, indicated the isopropyl group to be intact (as denoted by the *m/z* 197 ion generated from the characteristic loss of 42 Da).

Metabolite M11

Metabolite M11 was detected in radiochromatograms from monkey hepatocyte extracts only. Reverse-phase LC/radiometric analysis showed metabolite M11 to elute with a retention time of 21.1 min (Figure 2C). Metabolite M11 is proposed to consist of a combination of the hydroxylation of the ethylbenzene moiety and hydrolysis of an undetermined bond of the aminouracil moiety. The $[M+H]^+$ *m/z* 310 ion observed at the retention time of the radiolabelled metabolite M11 is consistent with the proposed structure (Figure 3). The LC-MS/MS characterization metabolite M11 is described below regarding the corresponding LC-MS/MS analysis of the unlabelled derivative. LC-MS/MS analysis of metabolite M11 provided informative characteristic fragmentation patterns in its MS/MS and MS^3 spectra (Supplemental Online Material Figure 7) that are similar to mavacamten and helped to identify the sites of metabolism. Tandem mass spectrometry of unlabelled M11 by collision-induced dissociation of

the parent protonated molecular ion leading to loss of water (loss of 18 Da) and the isopropyl (loss of 42 Da) gave rise to an *m/z* 248 fragment ion. A fragment ion at *m/z* 121 (originating from cleavage of the nitrogen-carbon bond) signified hydroxylation of the ethylbenzene moiety, while the remaining aminouracil portion of the metabolite, minus water (−18 Da), was represented by the *m/z* 170 ion. Further loss of the isopropyl from the *m/z* 170 fragment ion gave rise to an *m/z* 128 ion in the MS^3 spectrum.

Metabolite M13

Metabolite M13 was detected in radiochromatograms only from monkey hepatocyte extracts. Reverse-phase LC/radiometric analysis showed metabolite M13 to elute with a retention time of 31.0 min (Figure 2C). M13 is proposed to be the glucuronide of a mono-hydroxylated metabolite of mavacamten, the location of the hydroxylated carbon atom being on the uracil moiety. A protonated molecular ion $[M+H]^+$ *m/z* 468 observed at the retention time of radiolabelled metabolite M13 is consistent with the proposed structure (Figure 3). The LC-MS/MS characterization metabolite M11 is described below regarding the corresponding LC-MS/MS analysis of the non-radiolabelled derivative. LC-MS/MS analysis of metabolite M13 provided informative characteristic fragmentation patterns in its MS/MS and MS^3 spectra (Supplemental Online Material Figure 8) that are similar to mavacamten and assisted in the identification of the sites of metabolism. Cleavage of the carbon-nitrogen bond separating the ethylbenzene and aminouracil moieties results in the *m/z* 105 (ethylbenzene) and *m/z* 362 ions. A tandem fragmentation loss of the glucuronide (−176 Da) gives rise to the *m/z* 290 fragment ion, while the subsequent loss of the isopropyl, ethylbenzene and isopropyl plus ethyl benzene result in the *m/z* 248, 186 and 144 fragment ions, respectively. Further the *m/z* 424 ion represents the loss of

the isopropyl group (−42 Da). Together, these data confirmed that the site of hydroxylation is not on the isopropyl nor ethylbenzene moieties. Since a direct glucuronide of mavacamten has not been observed, the hydroxyl group of a mono-hydroxylated metabolite is assumed to be the site of glucuronidation.

CYP450 reaction phenotyping

Incubation of mavacamten (1 µM) with a range of human-recombinant cDNA-expressed enzymes (150 pmol/mL, 1 h) indicated the primary enzymes responsible for the metabolic depletion of mavacamten to be CYPs 2C19, 3A4 and 3A5 (Figure 5). CYP2C19 (28% parent mavacamten remaining) was responsible for the largest consumption of mavacamten, followed by CYP3A4 (56.4% parent mavacamten remaining) and CYP3A5 (42.8% parent mavacamten remaining). Incubations with human recombinant CYP isoforms 2C8, 2C9, and 2D6 resulted in a reduction of approximately 20% of mavacamten. The CYP reaction phenotyping results from mavacamten metabolite identification from incubations with selected individual CYP isoforms showed that metabolite M1 was primarily formed by CYP2C9*1 and metabolite M2 was primarily formed by CYP2C19 (data not shown). In addition, to a much lesser extent, CYP3A4 and CYP3A5 also contributed to the formation of M2. Metabolite M6 was formed primarily by CYP3A4 and CYP3A5 isoforms (data not shown).

Pre-clinical species pharmacokinetics of mavacamten

Representative pharmacokinetic parameters for mavacamten following single intravenous and oral dosing of mavacamten to male C57/BL6 mouse, Sprague-Dawley rat, beagle dog and

cynomolgus monkey are presented in Table 5. In all species studied, concentration-time profiles resulting from bolus intravenous administration are characterized by a rapid distribution phase followed by a terminal elimination phase with monoexponential decay (Figure 6). The intravenous clearance of mavacamten is low, at 2% of liver blood flow in the dog, and ranges from 7% to 10% of liver blood flow in mouse, rat and monkey. Mavacamten also displays a high volume of distribution (ranging from 3.8 L/kg in mouse to 10.6 L/kg in monkey) and long terminal $t_{1/2}$ (ranging from 6.9–130 h) across species (Table 5). Following oral administration, mavacamten had a $t_{1/2}$ ranging from 4.8–161 h (Table 5). The maximum concentration of drug following oral absorption was observed between 0.3 and 0.7 h, with a mean dose-normalised C_{max} ranging from 63 ng/mL in monkey to 564 ng/mL in mouse. The oral bioavailability when administered as a solution or highly dispersed suspension was high and ranged from 47% in monkey to 146% in mouse. This absorption profile is consistent with classification of mavacamten as Class II in the biopharmaceutical classification system, i.e., low solubility (0.02 mg/mL) and high permeability. The $t_{1/2}$ of mavacamten was similar between intravenous and oral dosing for each species tested.

Routes of elimination in rat

Following a single intravenous dose of [^{14}C]mavacamten (1 mg/kg) to BDC SD male rats (data not shown), the mean total recovery of radioactivity was 94.0 ± 0.3%. Radioactivity was eliminated rapidly, with approximately 70% of the administered radioactive dose recovered by 48 h post-dose. Excretion in bile accounted for approximately 41% of the administered radioactivity and was the predominant route of elimination. Urinary and fecal excretion accounted for approximately 31 and 8% of the administered dose,

respectively. At 96 h post-dose, approximately 7.9% of the administered dose was recovered in the residual carcasses. LC/radiometric analysis indicated that excreted drug-related radioactivity of AUC pooled (0-96 h) urine and bile was primarily in form of metabolites, where [^{14}C]mavacamten accounted for 8 and 3% of the total radioactive LC/radiometric-chromatographic peak area, respectively (data not shown). The major metabolite detected in urine was M4 (M1-glucuronide, 33% relative peak area to total), and the major metabolites detected in bile were M1 (23% relative peak area to total) and M4 (25% relative peak area to total).

Interspecies simple allometric scaling of CL and Vd_{ss}

Assuming a one-compartment model, for the prediction of mavacamten human pharmacokinetics, plasma pharmacokinetic parameters of CL and Vd_{ss} obtained from preclinical intravenous pharmacokinetic studies were transformed to unbound whole blood pharmacokinetic parameters for use in simple allometric interspecies scaling. The scaled human pharmacokinetic unbound whole blood parameters were then converted back to plasma pharmacokinetic parameters for direct comparison to pre-clinical species plasma pharmacokinetics. Through the use of simple allometric scaling of unbound blood clearance from mouse, rat, dog and cynomolgus monkey, the predicted human plasma clearance of mavacamten was 0.51 mL/min/kg (Table 6) with an allometric exponent of 0.725 (Figure 7). Employing the 'rule of exponents' (Mahmood and Balian 1996), the MLP correction is used when the allometric exponent from simple allometric scaling is equal to or greater than 0.7 and less than 1. Thus, when the MLP correction was used in this analysis, the allometric scaled CL_p was predicted to be 0.24 mL/min/kg, which was ~2-fold lower clearance than predicted by the

four-species simple allometric scaling method. When using a single-species liver blood flow method (Ward and Smith 2004), the predicted human mavacamten plasma clearance from comparison to rat, dog and monkey was 1.4, 0.4, and 1.4 mL/min/kg, respectively. The prediction of human Vd_{ss} is known to be successful using a simple allometric scaling method (Mahmood and Balian 1996). In the present work, as for CL, the Vd_{ss} of mavacamten in human was predicted using simple four-species allometric scaling of unbound blood Vd_{ss}. The predicted $Vd_{ss,p}$ of mavacamten in human is 9.5 L/kg (Table 6).

Discussion

Currently used medications for patients with HCM consist of 'off-label' drugs that are useful at reducing symptoms but do not treat the underlying cause of the disease. Mavacamten is a sarcomere modulator acting through direct binding to myosin, the motor protein of the cardiomyocyte. Mavacamten has been designed to treat the underlying cause of HCM by normalizing the function of myosin protein in hyper-contractile hearts.

The aims of the present studies were to understand the pharmacokinetics, *in vitro* biotransformation across species, and CYP450 drug-drug interaction potential of mavacamten in support of its progression into human. In these studies, mavacamten was administered to mouse, rat, dog and monkey by intravenous and oral administration in order to elucidate the intrinsic pharmacokinetic properties of mavacamten. **The intravenous pharmacokinetics of mavacamten across species demonstrated a 2-compartment model in each species tested.** The CL_p of mavacamten was low in the four species examined, ranging from 1.5% liver blood flow in dog to 10% liver blood flow in mouse. The volume of distribution was high across species and ranged from ~15-fold to ~5-fold total body water in monkey and mouse,

respectively. The terminal elimination $t_{1/2}$ was moderate in mouse (6.9 h) and rat (11.2 h); however, longer in the dog (130 h) and monkey (45 h). The binding to plasma protein was determined to be moderate to high and ranged from 84% to 97% in pre-clinical species and ~93% in human plasma. The oral bioavailability of mavacamten in pre-clinical species ranged from ~46% in monkey to greater than 100% in mouse.

Mavacamten demonstrated high apparent permeability in Caco-2 cells, predictive of good systemic oral absorption (Marino *et al.* 2005) and consistent with the high measured bioavailability in pre-clinical species. The drug showed an efflux ratio of 1.6, indicating a low potential for efflux transport of this passively permeable drug by transporters such as P-glycoprotein. With the combined high intrinsic permeability in Caco-2 cell monolayers and the excellent bioavailability observed in pre-clinical species, especially mouse, rat and dog, the bioavailability in human was predicted to be sufficient. From uptake studies with cryopreserved human hepatocytes, in the range of 0.5–100 μM, mavacamten uptake was not markedly different after 3 min at 37°C in the absence and the presence of a transporter 'inhibitor cocktail', i.e., where mean ratios between 1.2 and 1.5 were observed between the two conditions, indicating that transporters are probably not involved in mavacamten hepatic uptake.

***In vitro* metabolism studies showed mavacamten to be highly metabolically stable when exposed to liver microsomes from all species tested, where predicted CL_B values were less than 20% of liver blood flow. These results are consistent with the drug's low clearance observed *in vivo* in preclinical species. Due to the observed high metabolic stability *in vitro, in vivo* clearance data from preclinical species and allometry were used to project human clearance as discussed below.**

The *in vitro* metabolism of mavacamten was investigated using hepatocytes from Sprague-Dawley rat, beagle dog, cynomolgus monkey and human. Results from incubations with human hepatocyte demonstrated metabolites to be M1, produced from para-hydroxylation of the phenyl-moiety primarily generated by CYP2C9, a second oxidized metabolite, M2, which was obtained from terminal hydroxylation of the isopropyl moiety and proposed to be mediated by CYP2C19, and the metabolite M6, generated via CYP3A4/5-mediated *N*-dealkylation of the phenylethyl group. Additional metabolites detected in incubations with hepatocytes included metabolite M4 (the ether-linked glucuronide of M1 observed only in rat hepatocyte incubations), **M10 (formed only in rat hepatocytes and with an uncharacterized structure but where the net elements of $C_4H_6O_2$ are proposed to be added to the aminouracil moiety)**, M11 (detected only in monkey hepatocyte incubations and demonstrating metabolism of both the ethylbenzene and aminouracil moieties) and metabolite M13 (a glucuronide of an oxidized metabolite of the aminouracil moiety of uncharacterized structure and only observed in incubations with monkey hepatocytes). No glucuronide metabolites (direct nor phase II) were observed in human hepatocyte incubations with mavacamten, where M1, M2 and M6 were the sole metabolites detected, each in low abundance, and therefore, the metabolic clearance of mavacamten in human is predicted to be due to CYP-mediated metabolism.

Results from a rat BDC study indicated that [^{14}C]mavacamten-associated radioactivity measured in rat urine and bile represented approximately 31 and 41% of administered dose with a combined recovery of 72%. From this excreted radioactivity, only 8% (urine) and 3% (bile) of the total LC/radiometric peak area was represented by parent [^{14}C]mavacamten, indicating metabolic clearance to predominate in the elimination of the drug. From preliminary observations, the major metabolites detected in urine and bile

from rat were M4 (M1-glucuronide) in urine, and M1 and M4 in bile, which is consistent with the major metabolites detected in incubations with rat hepatocytes (Table 5). A comprehensive examination of metabolites detected in rat plasma and excreta is in progress.

Allometric scaling for the prediction of human CL and Vd_{ss} of mavacamten was based on interspecies simple allometric scaling of mouse, rat, dog and cynomolgus monkey intravenous pharmacokinetic parameters (Boxenbaum 1982). **Since the distribution phase rates of mavacamten far exceeded the terminal elimination rates for each of the preclinical species tested, we assumed a one-compartment model for the prediction human pharmacokinetics (Smith *et al.* 2018).** Prediction of human CL was performed by extrapolating pre-clinical species' unbound blood intravenous clearance, calculated based on experimental determination of plasma protein binding fraction unbound (fu_p) and blood-to-plasma ratio for each species, including human. Results from this simple allometric scaling method provided a CL_p of 0.51 mL/min/kg with an allometric exponent of 0.73. The 'rule of exponents' (Mahmood and Balian 1996) was examined in the current prediction, where it has been proposed that when the exponent of simple allometry lies between 0.71 and 0.99, allometric scaling of CL x MLP, a correction factor to normalize for metabolic capacity between species, would provide better predicted clearance compared with simple allometry alone. When MLP values (Nagilla and Ward 2004, Tang and Mayersohn 2005) for mouse, rat, dog, monkey and human of 2.8, 5.2, 18.4, 22.3 and 93.4 years, respectively, were used, the predicted CL_p in human was 0.24 mL/min/kg. Further prediction of clearance of mavacamten was performed by a method where clearance, predicted as percentage of liver blood flow in preclinical species, was used to predict human clearance (Ward and Smith 2004). By this method, the predicted mavacamten CL_p in

human ranged from 0.41 mL/min/kg from dog to 1.4 mL/min/kg from rat and monkey. Investigations by Ward and Smith (2004) suggested that monkey was the most predictive species when using this method.

In a similar manner, simple allometric scaling was employed to predict human mavacamten Vd_{ss}. This method has been used successfully for varied drugs (Ward and Smith 2004, McGinnity *et al.* 2007). Simple allometric scaling of unbound blood Vd_{ss} from mouse, rat, dog and monkey led to a predicted $Vd_{ss,p}$ of 9.5 L/kg. **The observed large Vdss cross-species is proposed to be due to binding to cardiac and skeletal muscle tissues (both containing mavacamten target protein). Based on the combination of available data we concluded that simple allometric scaling of volume of distribution across species is adequate for predicting mavacamten human volume of distribution.** The $t_{1/2}$ of mavacamten in human was predicted to be 214 h from simple allometric scaling and ranged from 463 h when employing the MLP correction for CL_p to 78.4 h when using predicted mavacamten human plasma clearance from single-species liver blood flow method compared with monkey. Based on mouse, rat, dog and cynomolgus monkey mavacamten oral bioavailability, a mean calculated oral bioavailability of 89% led to a predicted oral clearance of mavacamten of 0.58 mL/min/kg from simple allometric scaling, which ranged from 0.27–1.6 mL/min/kg from MLP correction allometric scaling and single-species liver blood flow methods, respectively. Similarly, simple allometric scaling of unbound blood mavacamten cross-species led to predicted mavacamten plasma $Vd_{ss,p}$ of 9.5 L/kg and predicted apparent oral plasma $Vd_{ss,p}$ of 10.7 L/kg.

Data from *in vitro* studies conducted in human liver microsomes indicate that mavacamten is not likely to be an inhibitor of CYP450 enzymes *in vivo* in human, and is therefore not likely to elicit drug-drug interactions through CYP inhibition. **However, *in vitro***

studies in human hepatocytes indicate the potential to induce CYP450 enzymes 2B6 and 3A4, which suggest the potential of mavacamten to affect the clearance of co-administered drugs metabolized by these enzymes. Some data from a mavacamten clinical study suggest that the risk of CYP induction is low. The plasma levels of 4β-hydroxycholesterol, which is considered as an endogenous biomarker for CYP3A4 (Mao *et al.* 2017), were measured from a multiple dose study in human volunteers. The data indicated no difference in 4β-hydroxycholesterol plasma levels after multiple dose treatment with mavacamten (data not shown), suggesting no change in CYP3A4 activity after treatment with mavacamten. Further work, including a clinical DDI study, are ongoing to fully characterize the potential of mavacamten to induce CYP3A4 in humans.

In summary, mavacamten is a first-in-class small molecule allosteric modulator for the inhibition of beta cardiac myosin currently under development for the treatment of HCM. The pre-clinical attributes and pharmacokinetics of mavacamten supported its progression into clinical investigations.

Acknowledgements

The authors thank the DMPK, Chemistry, and Analytical Formulations Departments at MyoKardia for their contributions to the results presented.

Disclosure of Interest

The authors are employees and stockholders of MyoKardia, Inc. and Sanofi.

References

Boxenbaum H. 1982. Interspecies scaling, allometry, physiological time, and the ground plan of pharmacokinetics. J Pharmacokinet Biopharm 10(2):201–27.

Brown RP, *et al.* 1997. Physiological parameter values for physiologically based pharmacokinetic models. Toxicol Indust Health 13(4):407–84.

Davies B, Morris T. 1993. Physiological parameters in laboratory animals and humans. Pharm Res 10(7):1093–95.

Gersh BJ, *et al.* 2011. 2011 ACCF/AHA guideline for the diagnosis and treatment of hypertrophic cardiomyopathy: a report of the American College of Cardiology Foundation/American Heart Association Task Force on Practice Guidelines. Circulation 124(24):e783–831.

Green EM, *et al.* 2016. A small-molecule inhibitor of sarcomere contractility suppresses hypertrophic cardiomyopathy in mice. Science 351(6273):617–21.

Hershberger RE, Cowan J, Morales A, Siegfried. 2009. Progress with genetic cardiomyopathies: screening, counseling, and testing in dilated, hypertrophic, and arrhythmogenic right ventricular dysplasia/cardiomyopathy. Circ Heart Fail 2(3):253–61.

Mahmood I, Balian JD. 1996. Interspecies scaling: a comparative study for the prediction of clearance and volume using two or more than two species. Life Sci 59(7):579–85.

Mao J, Martin I, McLeod J, Nolan G, van Horn R, Vourvahis M, Lin YS. 2017. Drug Metab Rev 49(1): 18–34.

Marino AM, Yarde M, Patel H, Chong S, Balimane PV. 2005. Validation of the 96 well Caco-2 cell culture model for high throughput permeability assessment of discovery compounds. Int J Pharm 297(1–2):235–41.

Maron BJ. 2002. Hypertrophic cardiomyopathy: a systematic review. JAMA 287(10):1308–20.

Maron BJ, Gardin JM, Flack JM, Gidding SS, Kurosaki TT, Bild DE. 1995. Prevalence of hypertrophic cardiomyopathy in a general population of young adults. Echocardiographic analysis of 4111

subjects in the CARDIA Study. Coronary Artery Risk Development in (Young) Adults. Circulation 92(4):785–89.

McGinnity DF, Collington J, Austin RP, Riley RJ. 2007. Evaluation of human pharmacokinetics, therapeutic dose and exposure predictions using marketed oral drugs. Curr Drug Metab 8(5):463–79.

Nagilla R, Ward KW. 2004. A comprehensive analysis of the role of correction factors in the allometric predictivity of clearance from rat, dog, and monkey to humans. J Pharm Sci 93(10):2522–34.

Obach RS. 1999. Prediction of human clearance of twenty-nine drugs from hepatic microsomal intrinsic clearance data: An examination of in vitro half-life approach and nonspecific binding to microsomes. Drug Metab Dispos 27(11):1350–59.

Poirier A, Lavé T, Portmann R, Brun ME, Senner F, Kansy M, Grimm HP, Funk C. 2008. Design, data analysis, and simulation of in vitro drug transport kinetic experiments using a mechanistic in vitro model. Drug Metab Dispos 36(12):2434–44.

Semsarian C, Ingles J, Maron MS, Maron BJ. 2015. New perspectives on the prevalence of hypertrophic cardiomyopathy. J Am Coll Cardiol 65(12):1249–54.

Smith DA, Beaumont K, Maurer TS, Di L. 2018. Relevance of half-life in drug design. J Med Chem 61(10):4273-82.

Tang H, Mayersohn M. 2005. A mathematical description of the functionality of correction factors used in allometry for predicting human drug clearance. Drug Metab Dispos 33(9):1294–96.

Walsky RL, Obach RS. 2004. Validated assays for human cytochrome P450 activities. Drug Metab Dispos 32(6):647–60.

Ward KW, Smith BR. 2004. A comprehensive quantitative and qualitative evaluation of extrapolation of intravenous pharmacokinetic parameters from rat, dog, and monkey to humans. II. Volume of distribution and mean residence time. Drug Metab Dispos 32(6):612–19.

Yu S, Li S, Yang H, Lee F, Wu J-T, Qian MG. 2005. A novel liquid chromatography/tandem mass spectrometry based depletion method for measuring red blood cell partitioning of pharmaceutical compounds in drug discovery. Rapid Commun Mass Spectrom 19(2):250-54.

Tables:

Table 1. Mavacamten plasma protein binding, blood-to-plasma ratio, and CL_{pred} across species.

Species	Plasma protein binding (% bound) at varied [mavacamten] 0.2 µM/1 µM/ 10 µM	Plasma protein binding (fu_p) at varied [mavacamten] 0.2 µM/ 1 µM/ 10 µM	Blood-to plasma ratio (mean ± SD)	Metabolic stability in liver microsomes ($t_{1/2}$, min)	$CL_{pred,blood}$ calculated from liver microsomes (mL/min /kg)	$CL_{pred,plasma}$ calculated from liver microsomes (mL/min /kg)
Mouse	83.6/ 84.2/ 84.0	0.16/ 0.16/ 0.16	0.72 ± 0.10	**>124**	**<11.7**	**<16.3**
Rat	89.4/ 89.1/ 88.5	0.11/ 0.11/ 0.12	0.82 ± 0.11	**>124**	**<8.71**	**<10.6**
Dog	92.6/ 91.9/ 88.8	0.07/ 0.08/ 0.11	0.78 ± 0.14	**>124**	**<6.9**	**<8.8**
Monkey	96.9/ 96.5/ 91.9	0.03/ 0.04/ 0.08	0.82 ± 0.09	**nd**	**-**	**-**
Human	92.9/ 93.3/ 93.1	0.07/ 0.07/ 0.07	0.79 ± 0.12	**>124**	**<3.9**	**<4.9**

CL_{pred}, predicted clearance; fu_p, plasma protein binding fraction unbound; SD, standard deviation; $t_{1/2}$, half-life.

Table 2. Uptake of mavacamten into human hepatocytes.

[Mavacamten]	Uptake at 37 °C minus 'inhibitor cocktail'	Uptake at 37 °C plus 'inhibitor cocktail'	minus 'inhibitor cocktail'/plus 'inhibitor cocktail' mean uptake ratio
µM	Mean ± SD	Mean ± SD	Mean ± SD
0.5	17.3 ± 3.1	11.9 ± 3.1	1.5 ± 0.1
3	92.3 ± 18.9	60.5 ± 7.3	1.5 ± 0.2
10	228 ± 48.4	168 ± 20.1	1.4 ± 0.2
20	318 ± 41.7	252 ± 25.4	1.3 ± 0.0
30	412 ± 69.9	353 ± 46.2	1.2 ± 0.1

SD, standard deviation**.**

Table 3. Determination of EC_{50} and E_{max} values for CYP3A4, CYP2B6, and CYP1A2 induction mediated by mavacamten. Values represent mean ± SD (from n=3 donor human hepatocyte preparations).

CYP isoform	EC_{50} (μM)		E_{max}	
	mRNA	Activity	mRNA	Activity
3A4	2.2 ± 0.4	1.4 ± 0.5	9.3 ± 5.9	6.5 ± 2.8
2B6	5.1 ± 0.2	3.7 ± 0.6	6.8 ± 1.6	5.3 ± 2.2
1A2*	-	-	-	-
Positive Controls				
CYP isoform/ inducer	**mRNA (fold-induction *versus* vehicle control)**		**Activity (fold-induction *versus* vehicle control)**	
3A4/ rifampicin	**11.0 ± 7.0**		**7.5 ± 4.0**	
2B6/ phenobarbital	**12.6 ± 4.3**		**13.2 ± 6.2**	
1A2/ omeprazole	**38.7 ± 12.9**		**17.7 ± 7.6**	

CYP, cytochrome P450; EC_{50}, half-maximal effective concentration; E_{max}, maximal effect; SD, standard deviation. ***No observed effect of mavacamten on CYP1A2 induction.**

Table 4. Cross-species metabolic profile of [^{14}C]mavacamten following 4 h incubation with hepatocyte suspensions.

Component	Species			
	Rat	Dog	Monkey	Human
MYK-461	80.4	99.6	89.0	96.9
M1	2.84	-	1.76	0.780
M2	1.15	-	2.71	0.940
M4	9.01	-	-	-
M6	4.41	0.380	3.21	0.770
M10	0.790	-	-	-
M11	-	-	1.30	-
M13	-	-	2.04	-
Unknown	1.42	0.00	0.00	0.630
Total	100	100	100	100

Table 5. Mavacamten pharmacokinetic summary in pre-clinical species following intravenous or oral administration.

Preclinical species mavacamten intravenous administration pharmacokinetics					
Species	Dose (mg/kg)	$AUC_{0–inf}$ (ng•h/mL)	CL_p (mL/min/kg)	$Vd_{ss,p}$ (L/kg)	$t_{1/2}$ (h)
Mouse[a]	1	2180	7.71	3.77	6.94
Rat	1	2880 ± 262	5.82 ± 0.5	5.01 ± 0.7	11.2 ± 1.0
Dog	0.25	7330 ± 1444	0.584 ± 0.1	7.01 ± 2.7	130 ± 20.4
Monkey	0.25	1520 ± 494	2.98 ± 1.1	10.6 ± 2.1	44.5 ± 7.8

Preclinical species mavacamten oral administration pharmacokinetics							
Species	Dose (mg/kg)	T_{max} (hr)	C_{max} (ng/mL)	$t_{1/2}$ (h)	$AUC_{0–inf}$ (ng•h/mL)	$DNAUC_{0–inf}$ (ng•h/mL)	*F (%)*
Mouse[a]	1	0.5	564	4.75	3170	3170	146
Rat	2	0.7 ± 0.3	522 ± 93.4	8.2 ± 1.0	4310 ± 1099	2155 ± 549	74.8 ± 19.1
Dog	0.5	0.3 ± 0.0	186 ± 74.1	161 ± 74.1	13500 ± 2835	27,000 ± 5670	87.1 ± 8.7
Monkey	0.5	0.7 ± 0.3	63.0 ± 23.4	42.7 ± 6.1	1410 ± 464	2820 ± 928	46.5 ± 15.3

$AUC_{0–inf}$, area under the concentration–time curve from time 0 to infinity; CL_p, plasma clearance; SD, standard deviation; $t_{1/2}$, terminal elimination half-life; $Vd_{ss,p}$, steady-state plasma volume of distribution. C_{max}, maximum concentration; $DNAUC_{0–inf}$, dose-normalized $AUC_{0–inf}$; T_{max}, time of C_{max}.

[a]Composite data obtained from mean concentrations of three subjects.

Values are mean ± SD of three subjects.

Table 6. Interspecies scaling of mavacamten intravenous plasma clearance (CL_p) and volume of distribution at steady state ($Vd_{ss,p}$) by four-species simple allometry for human pharmacokinetics prediction.

Species	Body weight (kg)	CL_p (mL/min/kg)	$Vd_{ss,p}$ (L/kg)	Liver blood flow (mL/min/kg)	Blood-to-plasma ratio	Plasma protein binding (fu_p)
Mouse	0.02	7.7	3.77	90	0.72	0.16
Rat	0.25	5.8	5.01	85	0.82	0.12
Dog	10	0.58	7.01	30	0.78	0.11
Monkey	5	3.0	10.6	45	0.82	0.08
Human[a]	70	0.51	9.5	21	0.79	0.07

CL_p, mavacamten intravenous plasma clearance; $Vd_{ss,p}$, steady-state plasma volume of distribution.

[a]Predicted CL_p and $Vd_{ss,p}$ parameters; body weight and liver blood flow values obtained from Davies and Morris (1993) and Brown *et al.* (1997).

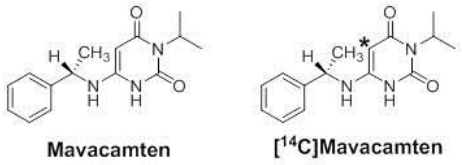

Figure 1

Figure 1. Structures of mavacamten, 6-([(1S)-1-phenylethyl]amino)-3-(propan-2-yl)-1,2,3,4-tetrahydropyrimidine-2,4-dione and [^{14}C]mavacamten (*denotes position of ^{14}C-label at the pyrimidine-5 carbon atom).

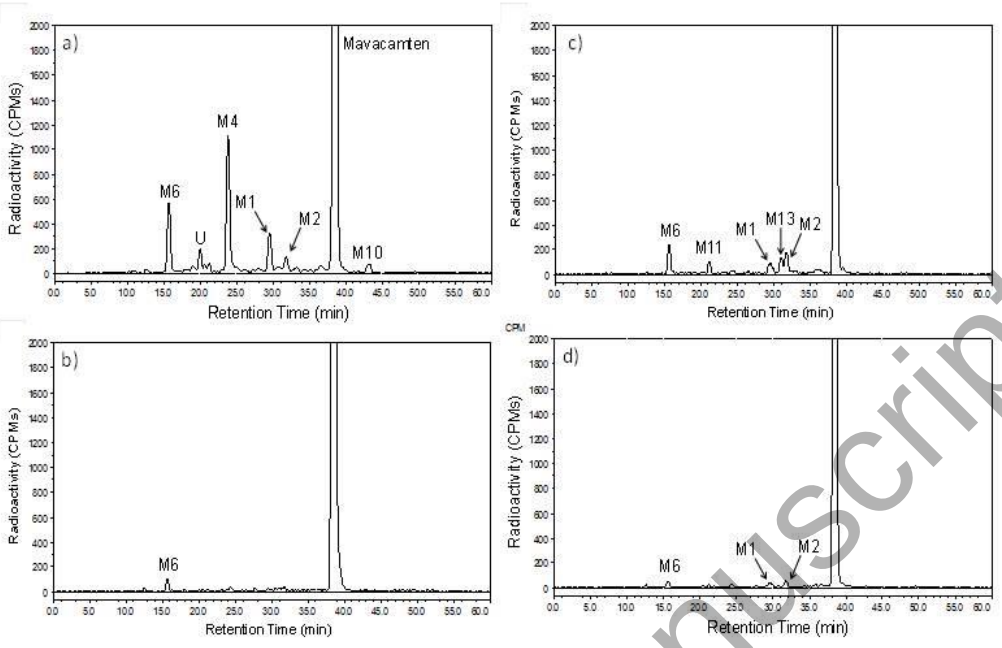

Figure 2

Figure 2. LC/Radioactivity chromatograms obtained from the analysis extracts from 4-h incubations of [^{14}C]mavacamten (10 μM) with hepatocytes from rat (A), dog (B), monkey (C), and human (D).

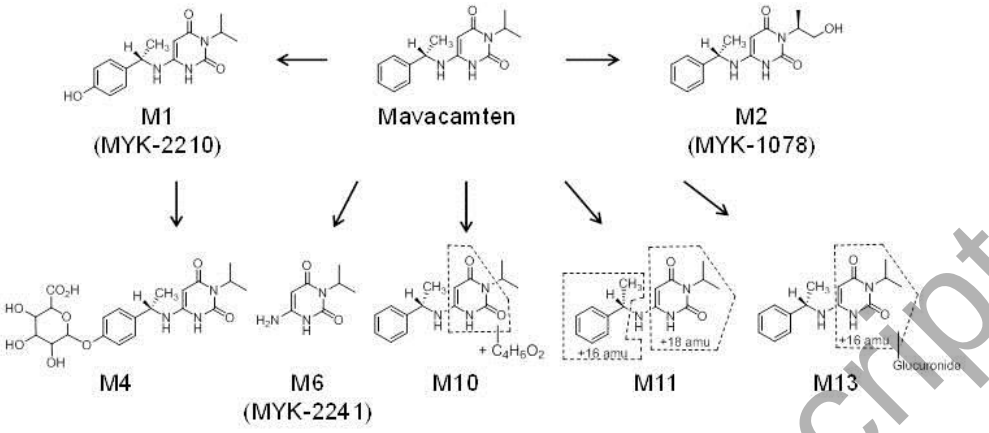

Figure 3

Figure 3. Scheme for the metabolism of mavacamten *in vitro* in hepatocytes.

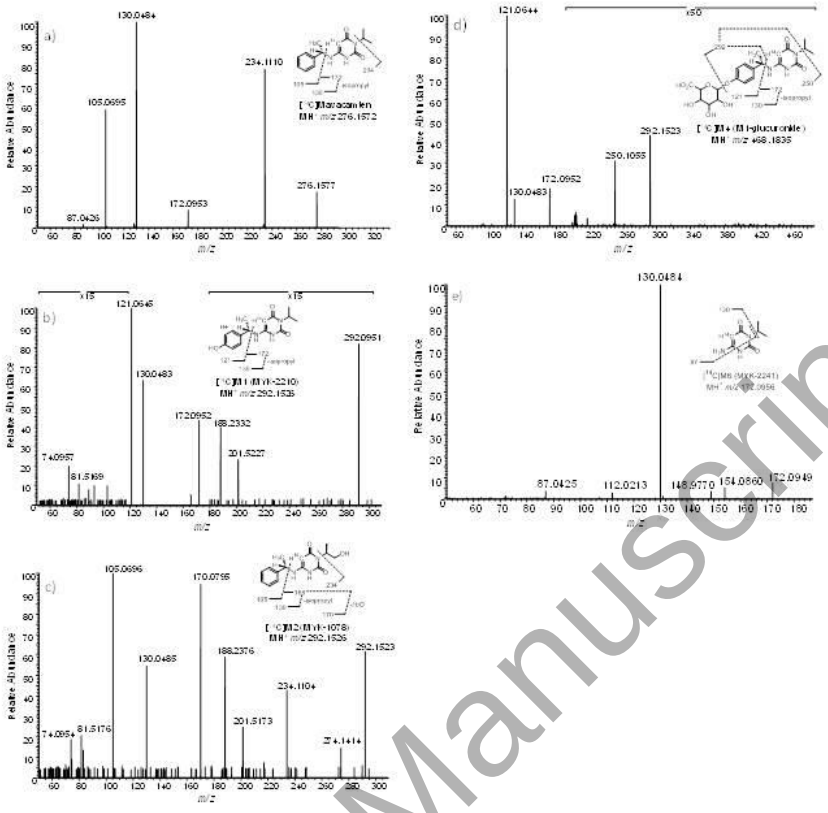

Figure 4

Figure 4. Positive ion LC-MS/MS analysis of (A) [^{14}C]mavacamten and the four major radiolabelled metabolites formed in hepatocyte incubations: (B) M1 (MYK-2210), (C) M2 (MYK-1078), (D) M4 (M1-glucuronide), and (E) M6 (MYK-2241).

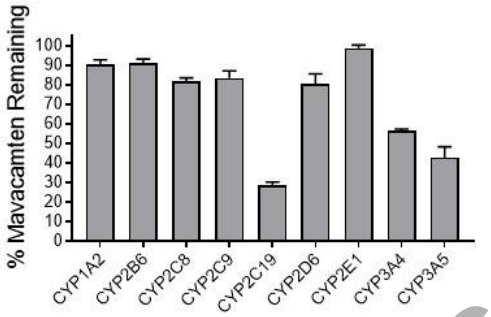

Figure 5

Figure 5. Metabolic stability of mavacamten (1 µM) in incubations with cDNA-expressed enzymes (150 pmol/mL) and NADPH for 60 min relative to mavacamten remaining in corresponding incubations lacking NADPH.

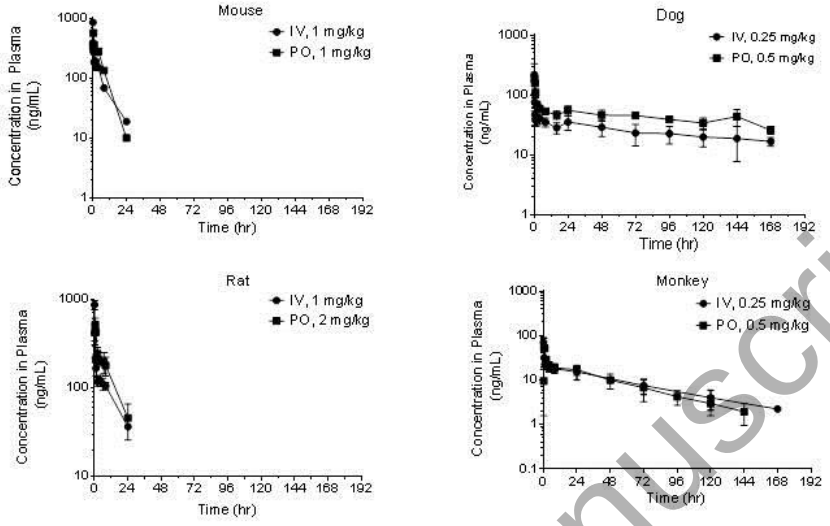

Figure 6

Figure 6. Cross-species concentration-time profiles of mavacamten post-administration intravenous or oral. Values are means ± SD, n=3.

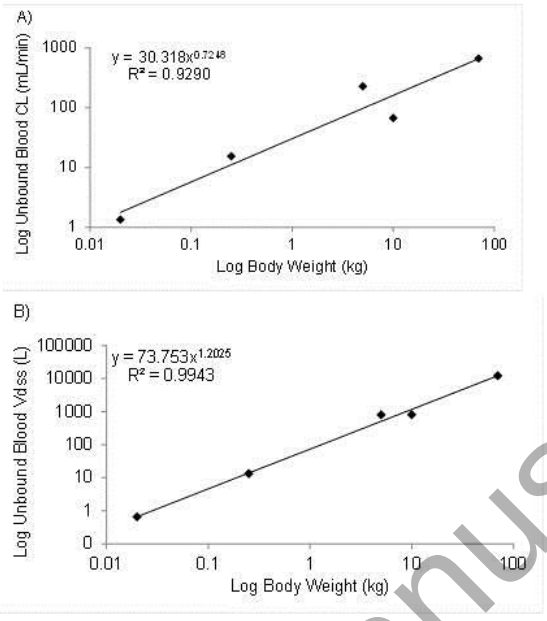

Figure 7

Figure 7. Simple allometric scaling of interspecies mavacamten (A) unbound blood CL and (B) unbound blood Vd_{ss} normalized to body weight.